frontiers | Frontiers in Materials

TYPE Original Research
PUBLISHED 23 August 2022
DOI 10.3389/fmats.2022.967871

Check for updates

OPEN ACCESS

EDITED BY
Bing Bai,
Beijing Jiaotong University, China

REVIEWED BY
Chen Peipei,
Beijing University of Civil Engineering and Architecture, China
Haiqing Zhang,
Hebei University, China

*CORRESPONDENCE
Wen-Chieh Cheng,
w-c.cheng@xauat.edu.cn

SPECIALTY SECTION
This article was submitted to Structural Materials,
a section of the journal *Frontiers in Materials.*

RECEIVED 13 June 2022
ACCEPTED 14 July 2022
PUBLISHED 23 August 2022

CITATION
Hu W, Cheng W-C, Wen S and Kang N (2022), Revealing underlying mechanisms affecting electrokinetic remediation of an artificially Cu- and Pb-contaminated loess using the external regulatory system with adsorbent.
Front. Mater. 9:967871.
doi: 10.3389/fmats.2022.967871

Revealing underlying mechanisms affecting electrokinetic remediation of an artificially Cu- and Pb-contaminated loess using the external regulatory system with adsorbent

Wenle Hu[1,2], Wen-Chieh Cheng[1,2,3]*, Shaojie Wen[1,2] and Nongbo Kang[1,2]

[1]Xi'an Key Laboratory of Geotechnical and Underground Engineering, Xi'an University of Science and Technology, Xi'an, China, [2]School of Civil Engineering, Xi'an University of Architecture and Technology, Xi'an, China, [3]Shaanxi Key Laboratory of Geotechnical and Underground Space Engineering (XAUAT), Xi'an, China

Considering extensive metallurgical mining activities in the northwest of China, handling Cu- and Pb-rich wastewater is a challenging task. Inappropriate handling of the Cu- and Pb-rich wastewater can lead to accumulation of Cu and Pb in the surrounding environment, thereby posing a serious threat to human health. Electrokinetic (EK) technology is an increasingly popular alternative to traditional approaches for contaminated soil remediation owing to its high effectiveness and low risk of secondary pollution. This study first proposed an external regulatory system with the adsorbent (ERSA) and investigated the effect of electrode type, ERSA, and cation exchange membrane (CEM) on the EK remediation of an artificially Cu- and Pb-contaminated loess. An EK reactor incorporating ERSA was applied to the EK experiments to circulate the electrolyte, not only making pH surrounding the cathode lower, but also preventing the formation of precipitation. The electrokinetic geosynthetics electrode released H^+ and OH^- faster and promoted their migration toward the specimen. However, because of the faster precipitation near the cathode, the boost in the remediation efficiency was hindered. Furthermore, considering the ERSA use, a decrease in soil pH near the cathode reduced the precipitation, thereby enhancing the EK remediation efficiency. In contrast, the use of CEM lowered the soil pH, increased the soil electrical conductivity (EC) and electric current, and aggravated the electroosmotic flow. The Cu remediation efficiency using the modified EK reactor was largely lifted to 85.52%, while the Pb remediation efficiency increased to 75.51%. These results shed light on an enhancement on the EK remediation efficiency and the potential of applying the modified EK reactor to remedy Cu- and Pb-rich water bodies.

KEYWORDS

loess soil, electrokinetic remediation, heavy metal, electrokinetic geosynthetics, external regulatory system with adsorbent

1 Introduction

With the rapid development of metallurgy, land contamination resulting from metallurgy industry wastewater poses serious threats to the surrounding environment and human health, raising sustainable development concerns. Heavy metals are major chemicals causing soil pollution. In the northwest (NW) of China, loess bears the greatest burden of environmental contamination (Hu et al., 2021a; Hu et al., 2021b). Because of industrial or agricultural waste, it is contaminated by various toxic elements such as copper, lead, mercury, cadmium, and arsenic (Saha and Orvig, 2011; Ghosh et al., 2015; Begum et al., 2022). Heavy metals are toxic, carcinogenic, and strongly adsorbed onto the loess, which can be transported into the human body and accumulated with time eventually affecting human, animal, and plant health (Bai et al., 2019, 2020; Bai et al., 2021c). More importantly, heavy metal contamination is difficult to handle because of its long residual time, strong concealment, toxicity, and other characteristics. Furthermore, artificial remediation or soil self-purification needs long time to degrade contaminants. The remediation of soil contaminated by heavy metals is still a challenge. Therefore, feasible and efficient measures for remediation of soil contaminated by heavy metals are necessary.

The currently available measures for the remediation of soil contaminated by heavy metals mainly include phytoremediation (Caparrós et al., 2022; He et al., 2022; Liu et al., 2022; Wu et al., 2022), thermal desorption (Ding et al., 2019; Liu et al., 2019, 2020), biosorption (Saha et al., 2011; Mukherjee et al., 2013), soil replacement (Du et al., 2011), curing stabilization (Kalantari and Prasad, 2014; Zhou et al., 2017; Wang et al., 2019), chemical precipitation (Lu Y. S. et al., 2019; Muddanna and Baral, 2019), and microbial remediation (Garcia-Sanchez et al., 2018; Lu C. et al., 2019; Wang et al., 2022a; Xue et al., 2022). Among the remediation measures, electrokinetic (EK) remediation has recently come under the spotlight and is considered a promising innovative remediation technology, especially for low permeability soils. Moreover, EK remediation displays better behaviors in terms of metal mobilization and low repeated contamination (Zhou et al., 2021) by inserting the electrodes into the soils and applying a low direct-current (DC) voltage gradient to the electrodes. During EK remediation, the applied electric gradient induces a pH gradient across the soil chamber because of water electrolysis reactions that produce protons at the anode and hydroxyl ions at the cathode. The process also leads to electric effects, including electroosmosis, electromigration, and electrophoresis. Among these, electroosmosis and electromigration are the main removal mechanisms in most instances (Beyrami, 2020; Zhou et al., 2021). Furthermore, the acidic environment generated at the anode aids in the desorption and dissolution of heavy metals from the soil particle surface. It is unfortunate that, the alkalization near the cathode is considered the main barrier to the migration of heavy metal ions from the soil. Moreover, it is not conducive to the desorption and migration of heavy metal ions because of the weak alkaline conditions of loess itself (Hu et al., 2021a), limiting the development and application of EK remediation technology. Moreover, loess is extremely important and covers 630,000 km^2 in China. Clay minerals in loess have complex chemical composition, high specific surface areas, and high negative charge (Xue et al., 2021a, 2021b; Duan et al., 2021; Bai B. et al., 2021, 2021b). The forming of water during the EK remediation process can cause the swelling and dispersion of clays in loess toward increasing the thickness of the electric double layer and causing a reduction in the suction (Hu et al., 2021a; Hu et al., 2022a; Wang et al., 2022a). The reduced suction deteriorates the metastable structure of the loess, accompanied by the collapse deformation (Wang et al., 2020; Hu et al., 2021a), which makes the channel of the pore decrease and further limits the application of EK remediation technology.

Previous studies have shown that the EK remediation technology has the potential to effectively remove heavy metals from soil (Chen et al., 2020; Wang et al., 2021), especially in sandy soil (Baker et al., 2018; Puppala et al., 1997), soft soil (Wang et al., 2021), black soil (Yuan et al., 2017), and kaolin (Li et al., 2019). A significant body of research conducted over the past few years has greatly improved our understanding of the removal of heavy metals and their influencing factors when using EK technology. For instance, Kim et al. (2005) evaluated the potential of EK technology enhanced by an ion-exchange membrane (IEM) for remediating heavy metal contaminated soils. The experimental results indicated that the effectiveness of EK technology was increased by an enhancement scheme using an IEM. Xu et al. (2020) found that applying the cation exchange membrane (CEM) to the cathode could increase the removal efficiency by decreasing soil pH near the cathode. Ling et al. (2021) confirmed the effectiveness and feasibility of electrokinetic geosynthetics (EKG) electrodes in long-term subgrade improvement technology based on electroosmosis. Compared to the traditional graphite electrode, both laboratory and field tests indicated that the EKG electrode is more suitable for long-term electroosmosis treatment because of the lower

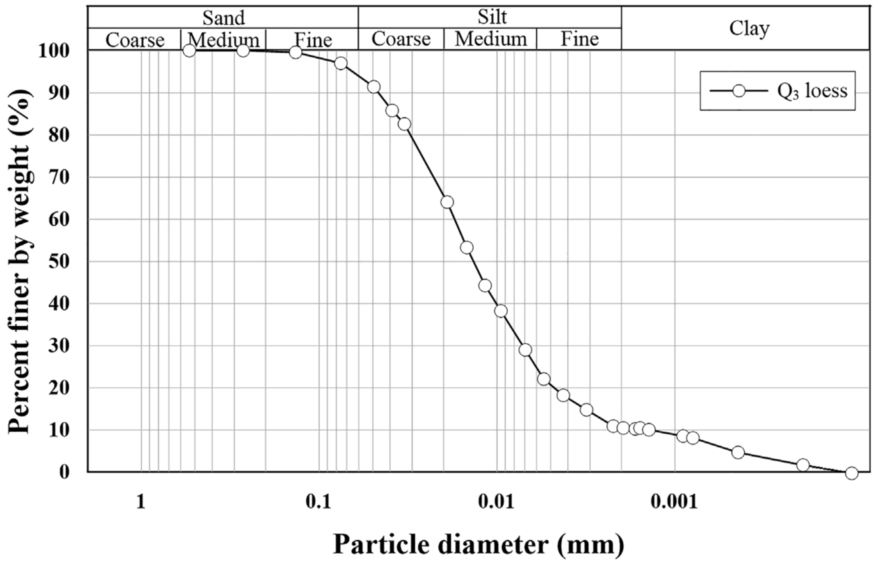

FIGURE 1
Particle-size distribution of the loess.

energy cost of the EKG electrode. Chang et al. (2018) proposed that applying the circulation-enhanced electrokinetic system can maintain a relatively neutral pH of treated soils and make the removal efficiency of Cd and Pb achieve 91 and 85%, respectively. Mohadi et al. (2019) illustrated that contaminated soil remediation could be affected by the operating conditions of the EK process, including pH control, refreshing electrolytes, and changing voltage gradient. Fan et al. (2021) found that the EK coupled with acidic permanganate of the regular oxidant supplement is appropriate for mass removal of heavy metals and polycyclic aromatic hydrocarbons, especially in low-buffered soils. Zhou et al. (2021) and Wang et al. (2021) noted that coupling the EK with other remediation technologies could improve the efficiency of EK remediation or decrease energy costs. Handling Cu- or Pb-rich wastewater, induced by metallurgical activities, is deemed a challenging task, especially in the NW of China. Permeation of Cu and Pb into ground soils can decrease plants' photosynthetic activities (Bilal et al., 2013; Mwandira et al., 2017; Meseldzija et al., 2019) and cause their accumulation. Their accumulation could lead to great harm to organisms or even to humans through food chain (Zu et al., 2004; Tak et al., 2013; Hu et al., 2021a; Hu et al., 2022b; Wang et al., 2022b).

A number of questions regarding the underlying mechanisms affecting the EK remediation efficiency remain (e.g., effect of electrode polarization, heavy metal precipitation surrounding the cathode, etc.). The main objectives of this study are 1) to investigate the effect of electrode types, the external regulatory system with adsorbent (ERSA), and CEM on the removal of copper and lead; 2) to reveal the underlying mechanisms affecting the EK remediation efficiency; and 3) to shed light on the potential of applying the modified EK reactor to remedying the Cu- and Pb-rich water bodies.

TABLE 1 Physicochemical properties of the loess.

Physical parameter	Value
Sand (%)	3.3
Silt (%)	87.4
Clay (%)	9.3
Void ratio, e	0.898
Bulk unit weight, γ (kN/m^3)	16.2
Specific gravity, G_s	2.69
Water content, ω_n (%)	16.5
Liquid limit, ω_L (%)	31.6
Plastic limit, ω_P (%)	19.5
USCS symbol	CL
Permeability (m s^{-1})	2.55×10^{-6}
Organic matter (mg g^{-1})	4.1
pH	8.3
Electrical conductivity (S m^{-1})	0.244
BET specific surface area (m^2 kg^{-1})	2.41×10^4
Ca^{2+} (mg/kg)	126
Mg^{2+} (mg/kg)	40
Na^+ (mg/kg)	103
K^+ (mg/kg)	4.6

TABLE 2 Experimental design of the enhanced electrokinetic remediation of Cu- and Pb-contaminated loess.

Test	Electrode type	Contaminant	Voltage gradient/V·cm^{-1}	Adsorbent	Catholyte	Cation exchange membrane
Exp-01	Graphite	Cu + Pb	1.5	/	/	/
Exp-02	EKG	Cu + Pb	1.5	/	/	/
Exp-03	EKG	Cu + Pb	1.5	Biochar	A to C	/
Exp-04	EKG	Cu + Pb	1.5	Graphene	A to C	/
Exp-05	EKG	Cu + Pb	1.5	Biochar	A to C	The cathode side
Exp-06	EKG	Cu + Pb	1.5	Graphene	A to C	The cathode side

"/" indicates that the corresponding test was not used in the treatment. "A to C" indicates that the anodic electrolyte was pumped out from the anodic chamber and injected into the cathode chamber using a peristaltic pump following adsorption of the adsorbing device.

2 Materials and methods

2.1 Sampling and specimen preparation

In NW China, dust and sand brought by wind are deposited in the Loess Plateau, and loess is formed after three stages of leaching, illuviation, and accumulation of the aeolian materials. There are three major geomorphologic features present in the Loess Plateau: loess ridges, hills, and bedrock gullies. Boreholes data indicate that the strata overlying the sandstone bedrock consist of Palaeosol and the overlying Malan (Q_3) loess, and their thickness varies between 22 and 31 m and 2 and 5 m, respectively (Zhu et al., 2011; Hu et al., 2021a). A series of Q_3 loess block samples from Lantian, Shaanxi Province, were used in this work, approximately 22 km southeast of Xi'an, with a sampling depth of 3.0–4.5 m. In addition, samples retrieved from the sampling site and used in this study have not detected Cu and Pb. The particle-size distribution curve of Q_3 loess is shown in Figure 1. The basic physical and chemical properties of the loess used in this study were determined immediately upon the delivery of the loess blocks according to the (Ministry of Water Resources of the People's Republic of China, 2019) and summarized in Table 1, such as initial water content, void ratio, pH, EC, and element composition.

Previous studies (Zeng et al., 2020; Zheng et al., 2021) have indicated that the process of loess contaminated by heavy metals causes changes in the microstructural characters because of the loess–water–chemical interactions. Furthermore, the process of EK remediation again changes the microstructure of the contaminated loess by the electroosmosis of pore water and electromigration of cations and heavy metal ions. Considering this, compared with the test on real contaminated matrices, the spiked matrices can better ensure the uniformity of the distribution of contaminants. They might be more appropriate in exploring the main contributor to the enhanced remediation efficiency and revealing the improved mechanism of leading the higher remediation efficiency. According to the National Bureau of Statistics (2001) data, Cu and Pb were selected as spiked contaminants for the soil treatment tests. The concentration of Cu and Pb was selected as 500 mg/kg, respectively, according to the previous study (Yuan et al., 2017; Zang et al., 2019) and the data of the National Bureau of Statistics (2018).

The natural loess was air-dried, pulverized, sieved (2 mm), and stored in a sealed glass cylinder. Our previous work took three degrees of compaction (0.8, 0.85, and 0.9) and three moisture contents (15, 20, and 25%) into account while remedying the Cu- and Pb-contaminated loess through the EK remediation technology. The experimental results indicated that the lower degree of compaction (i.e., 0.8) promoted the formation of the agglomerate structure, and therefore, causes the electromigration path wider and straighter, elevating the percentage removal of heavy metals. Furthermore, the slippage of the Gouy layer aggravates the electromigration of the cations and heavy metal ions when subjected to the higher initial water content (i.e., 25%), thereby enhancing the removal of heavy metals. These two parameters were subsequently applied to the testing scheme. The mass of the Cu nitrate [$Cu(NO_3)_2$] and Pb nitrate [$Pb(NO_3)_2$] with a purity >99% were calculated following the quality of air-dried loess. Then the Cu nitrate [$Cu(NO_3)_2$] and Pu nitrate [$Pb(NO_3)_2$] were dissolved in the given amount of deionized water. The solution containing copper and lead ions was sprayed into the loess in layers according to the Ministry of Water Resources of the People's Republic of China (2019). When the loess soil is exposed to a solution containing Cu and Pb ions, the initial adsorption reaction of heavy metals entering the soil is swift. This reaction is usually completed within a few hours and no longer exists later. The ecotoxicity of Cu and Pb in soil decreasing slowly with time is called aging treatment. The prepared Cu- and Pb-contaminated loess was sealed and stored in a moisturizing tank for 72 h to simulate the time effect of on-site contamination and ensure the even distribution of toxicity.

In all cases, the specimens were compacted in five layers to control the degree of compaction of contaminated loess on the reactor after aging treatment. After every layer preparation was completed, the surface of the layers was treated with a knife to make the two layers of soil come into close contact until the fifth

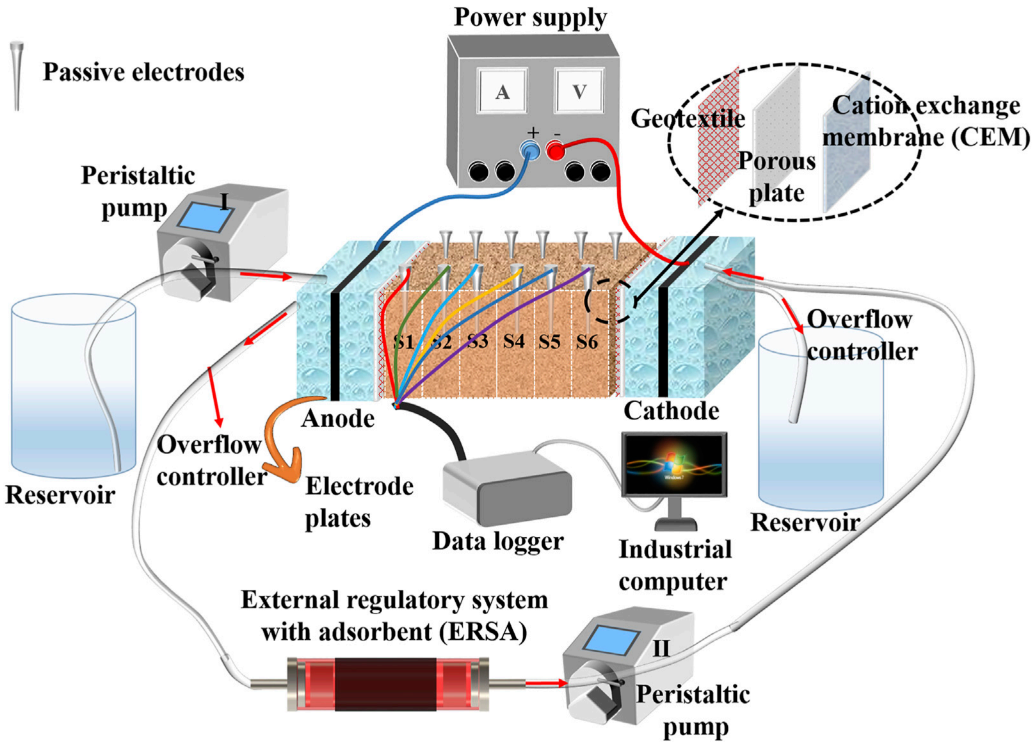

FIGURE 2
Schematic illustration of the electrokinetic reactor.

layer. The EK reactor and experimental details after the sample is prepared will be introduced in the following section.

2.2 Modified electrokinetic reactor and experimental design

A modified EK reactor applied to EK experiments in the present study mainly consists of one soil chamber made of plexiglass, two electrode cells, a pair of electrodes, two electrolyte reservoirs, two peristaltic pumps, one DC regulated power supply, the ERSA and data acquisition system, as shown in Figure 2. Dimensions of the soil chamber are 500 mm (length) × 150 mm (width) × 150 mm (height). Furthermore, the dimensions of the electrode cell are 100 mm (length) × 150 mm (width) × 150 mm (height). The two electrode cells are attached to both sides of the soil compartment containing six parts (termed S1 to S6 hereafter) and separated from the soil compartment using a geotextile and porous plate. The filling height of the soil in the soil chamber should be slightly higher than the liquid level of electrolyte in the electrode compartment, while the liquid level of electrolyte in the electrode compartment should be equal to the height of the lower end of the overflow controller. The setting of the overflow controller is used to ensure a constant liquid level of electrolyte in the electrode cell. A pair of electrodes were deployed to electrode compartments toward developing the electric field using a DC power supply. The two electrolyte reservoirs are connected respectively to the two electrode compartments. Moreover, the ERSA was used to adsorb the heavy metals in the anodic electrolyte and ensure that the purified anodic electrolyte was circulated the cathode cell using two peristaltic pumps. The two peristaltic pumps were opened throughout the EK remediation. The anodic electrolyte was circulated to the cathode cell to prevent pH surrounding the cathode from going higher. Measurements of pH, electrical conductivity (EC), electric current, and electroosmosis were done in each part (S1 to S6) using the data acquisition system during the EK remediation.

Material selection of the electrode itself is crucial in mitigating the effect of electrode polarization, and it has focused on EC and electrochemical activity. In light of this, higher current density and corrosion resistance were deemed as the main criteria for determining an appropriate material of electrodes applied to the EK remediation (Han et al., 2021; Wang et al., 2021). There are two types of electrodes present in this study: graphite and EKG (Wen et al., 2021). Both meet the said requirements. A pair of EKG electrodes were used as the modified electrodes, and a pair of graphite electrodes were

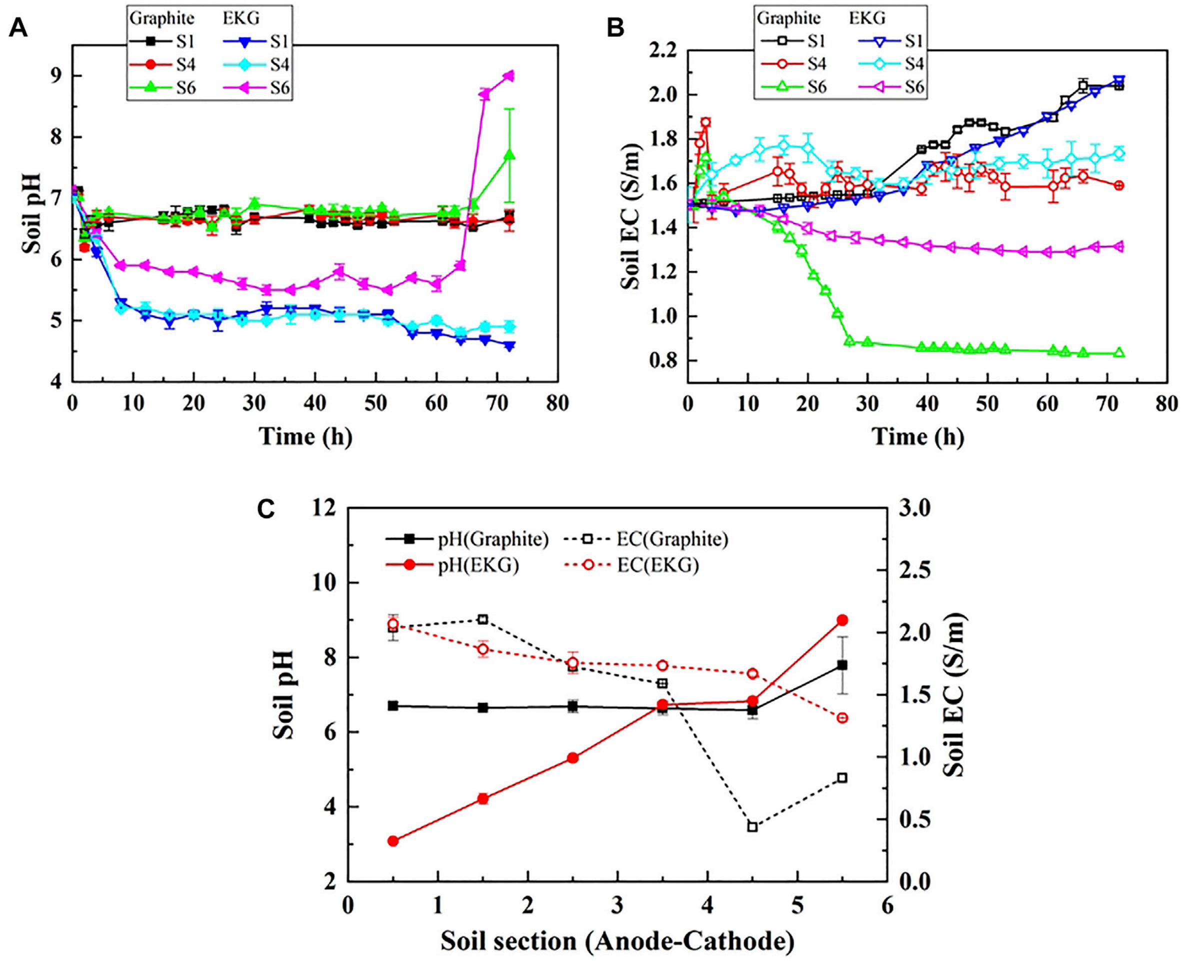

FIGURE 3
(A) soil temporal relationship, **(B)** soil EC temporal relationship, and **(C)** relationship of soil pH versus soil section.

used as the reference electrodes (see Table 2). According to the nitrogen adsorption method, it is essential to point out that the specific surface area (SSA) of the graphite electrode and EKG electrode was 1.12×10^3 m^2/kg and 8.90×10^3 m^2/kg, respectively. Furthermore, the theoretical SSA of graphene particles was nearly three times greater than biochar particles. The larger the SSA, the stronger the adsorption capacity. The adsorbent may affect the performance of the external regulatory system in the circulation of anolyte. To this end, two different types of high-efficiency adsorbents were considered, including biochar and graphene. Moreover, the CEM was used to evaluate its utility and mechanism in EK remediation. At the end of each EK experiment, the Cu and Pb removal was analyzed and compared against other EK experiments. All EK experiments had three replicates. An error bar has already been added to figures where necessary. Statistical analysis indicates that the coefficient of variance for the EK experiments is <15%, which is within the requirement being the coefficient of variance for usual, accessible experimental measurements.

3 Results

3.1 Effect of electrode type

Soil pH is a critical factor affecting the EK remediation efficiency. EK treatment changes pH through the electrolysis reaction at the electrodes and the migration of H^+ and OH^-. The changes of pH against different sections of the modified EK reactor applied to the present work are presented in Figure 3. Acar and Alshawabkeh (1993) found that the H^+ dominates the EK remediation efficiency because the mobility of H^+ is 1.75 times faster than that of OH^- (Bala et al., 2015). In the present work, the electrolysis unit consists of the electrodes for

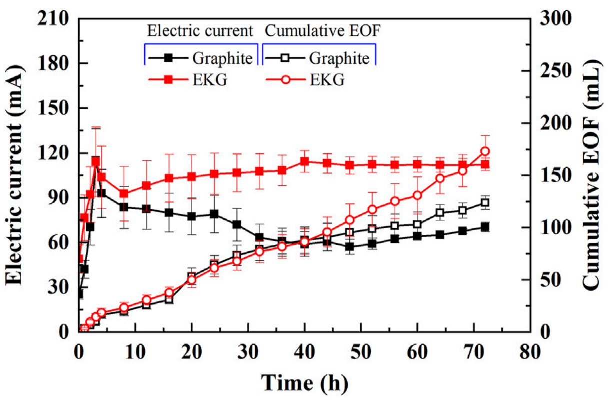

FIGURE 4
Variation of electric current and electroosmotic flow (EOF) versus time during the electrokinetic experiment subjected to the effect of electrode type.

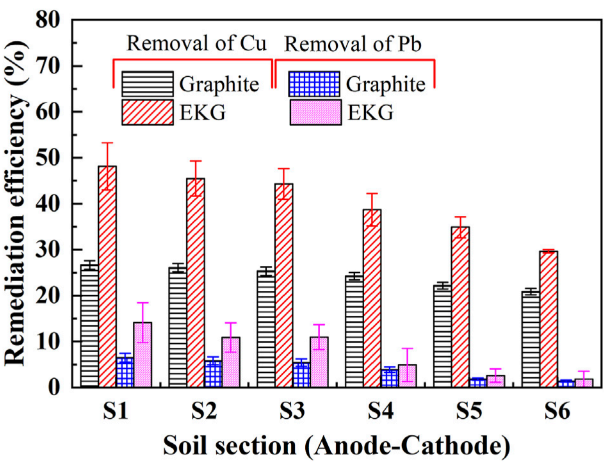

FIGURE 5
Removal of Cu and Pb after the electrokinetic experiment subjected to the effect of electrode type.

electrolysis, during which the modified EK reactor causes pH to increase sequentially from anode to cathode, while EC however behaves in a manner against pH (Figures 3A,B). When graphite is considered as the electrode, the pH surrounding the anode decreases to 6.70 and the pH surrounding the cathode increases to 7.79. Considering EKG as the electrode, the pH surrounding the anode decreases to 3.09 and the pH surrounding the cathode increases to approximately 9 (Figure 3C). Compared to the graphite electrode, the EKG electrode for a given soil section made pH surrounding the anode lower and the one surrounding the cathode remained nearly the same. This causes the hydrogen ions to adsorb on the soil particle surfaces, and the hydroxide ions leave behind, elevating pH surrounding the cathode. In contrast, the EC surrounding the anode is the highest and the one surrounding the cathode is the lowest. The acidic environment surrounding allows more ions to be desorbed from the loess, which causes EC to increase.

It is well known that the changes in the electric current and electroosmotic flow (EOF) have significant effects on the remediation efficiency of heavy metals. In general, the variation of electric current against the time can be characterized as two stages (Stages I and II) (Figure 4). Stage I can be characterized as an initially sharply increasing curve. Stage II can be described as a subsequently gently decreasing curve with the exception of EKG. H^+ ions and OH^- ions are discharged from the anode and cathode respectively throughout the EK remediation, which leads to an increasing number of ions migrated. Apart from that, H^+ also causes the soluble salts and minerals of the loess to dissolve, which further increases the number of ions migrated. The migration of H^+ promotes the desorption of heavy metals from the loess surface. Electric current increases quickly with the elapsed time as a result, as indicated by Stage I of Figure 4. The alkaline front is responsible for the precipitation surrounding the cathode, thereby causing the electrical resistance to increase and electric current to decrease. The electric current for EKG remains at a relatively high level, most likely because of the reduced effect of electrode polarization. Furthermore, gas bubbles, while using the graphite electrode, are constantly present on the electrodes' surface throughout the EK remediation, causing some difficulty in discharging more ions and lifting up EC. Moreover, the concentration polarization simultaneously presents in the anode and cathode cells, which also leads to a decrease in electric current. Compared to the graphite electrode, a higher SSA of the EKG electrode leads to lower current density on the surface and reduces the concentration polarization toward causing larger potential differences and higher EC. A higher electric current implies that H^+ and OH^- are discharged faster. These results provide testimony to the main cause leading to the EOF curve for EKG lying above the graphite curve, given a more significant heavy metal precipitation following a certain period of time (here it is 40 h) (Figure 4).

EOF depends highly on soil zeta potential, and the zeta potential depends on the interfacial chemistry between the pore fluid and particles. The zeta potential is negative under neutral and alkaline conditions (Acar and Alshawabkeh, 1993). As discussed, the EKG electrode causes H^+ and OH^- to be discharged manner and turns the most areas of the specimen into acidic environments, causing higher EC and EOF (Figure 4). Cationic metal is generally transferred to the cathode by electromigration and electroosmosis (Acar and Alshawabkeh, 1993). The Cu and Pb remediation efficiency against different soil sections is presented in Figure 5. Compared to the graphite electrode, the EKG electrode for a given soil section made

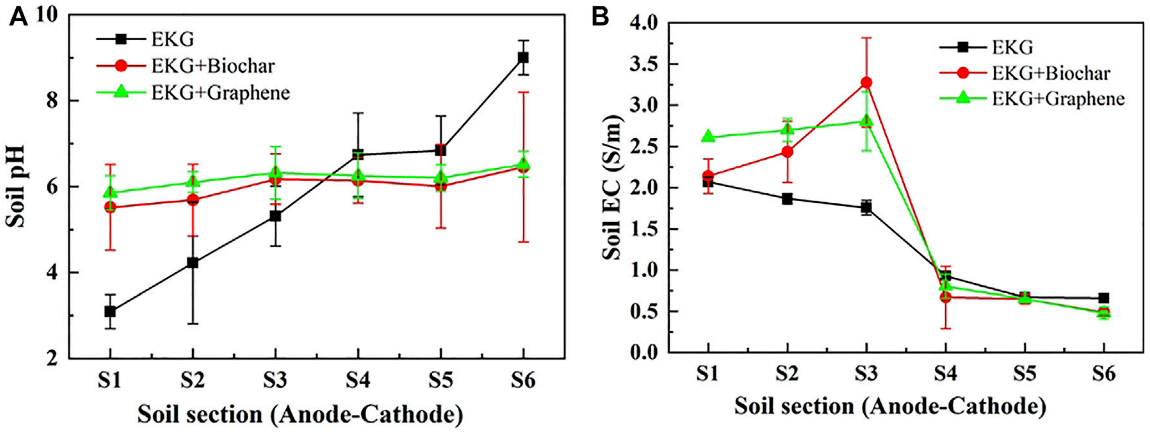

FIGURE 6
Variation of pH and EC after the electrokinetic experiment subjected to the effect of the adsorbed material: **(A)** pH and **(B)** EC.

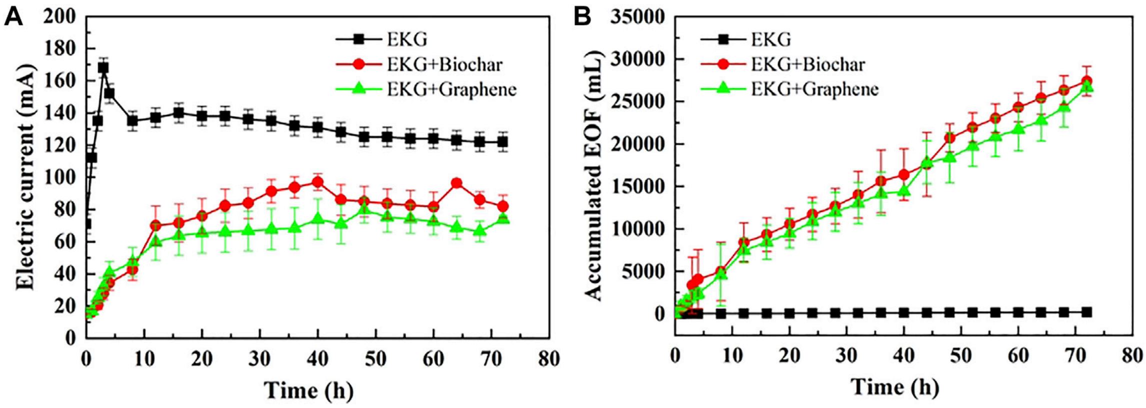

FIGURE 7
Variation of electric current and EOF versus time during the electrokinetic experiment subjected to the effect of the adsorbed material: **(A)** electric current and **(B)** accumulated EOF.

pH surrounding the anode lower. The migration of H^+ promotes the desorption of heavy metals from the surface of the loess improving the remediation efficiency. Such advantage is reduced with the increase in the distance from the anode. Furthermore, the Cu remediation efficiency is higher than the Pb remediation efficiency. Considering the ionic radius of Cu^{2+} is smaller than the ionic radius of Pb^{2+} (0.073 vs. 0.119 nm), the hydrated ion radius of Pb^{2+} is smaller than that of Cu^{2+}. That is, Pb^{2+} is much more difficult to desorb compared to Cu^{2+}. This is, therefore, deemed as the main cause that leads to the higher Cu^{2+} removal.

In short, pH surrounding conditions play a crucial role while introducing the EK remediation using the modified EK reactor. The EKG electrode makes H^+ and OH^- to be discharged faster compared to the graphite electrode, turning most areas of the specimen into acidic environments. The lower the pH surrounding, the more ions to be desorbed, and the higher the EC toward elevating EOF. Considering more cations are discharged while using the EKG electrode, the cations, in turn, reduce the zeta potential, forming an agglomerated structure. The agglomerated structure shortens the migration path of Cu^{2+} and Pb^{2+} and then elevates EOF and the remediation efficiency.

3.2 Effect of the external regulatory system with the adsorbent

Despite the advantages of the EKG electrode, precipitation surrounding the cathode is still notable, causing an inability of elevating the EK remediation efficiency. In the control group

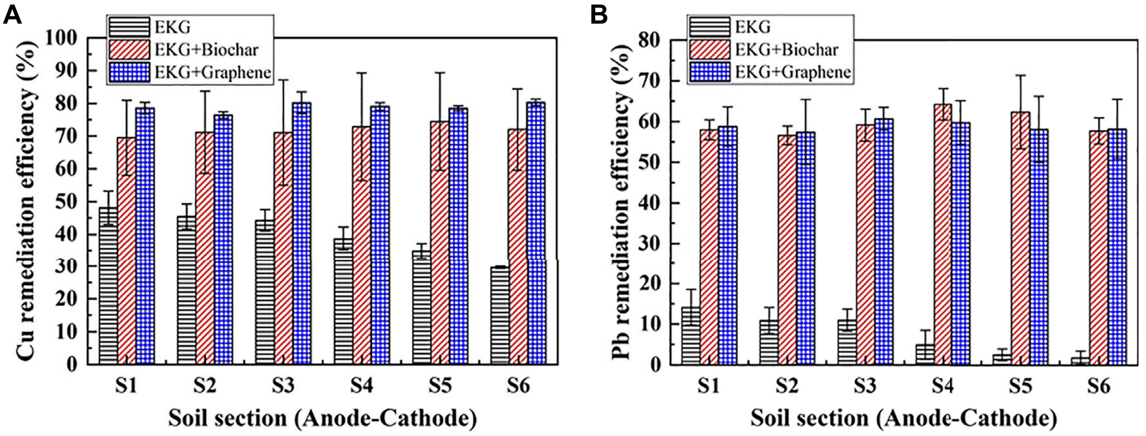

FIGURE 8
Removal of Cu and Pb after the electrokinetic experiment subjected to the effect of the adsorbed material: **(A)** Cu and **(B)** Pb.

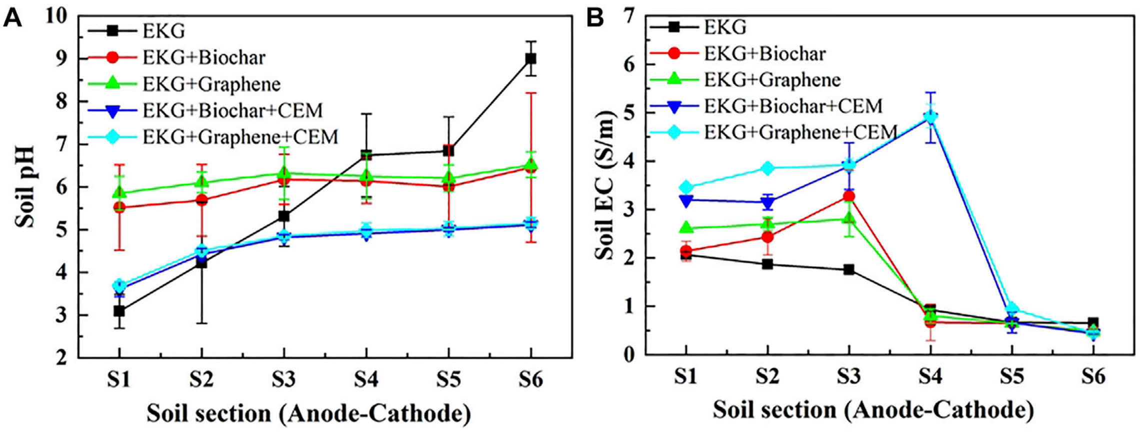

FIGURE 9
Variation of pH and EC after the electrokinetic experiment subjected to the effect of the different treatments: **(A)** pH and **(B)** EC.

(using EKG only), pH varies from 3.1 to 9.0 (Figure 6A). In the other test group (considering EKG and biochar), pH varies from 5.3 to 6.6, while in another test group (considering EKG and graphene), pH is further decreased. The increase in EC for the test groups is more significant compared to the control group, especially for the soil Sections S1–S4 (Figure 6B). These results provide testimony regarding the above argument.

The variation of electric current and EOF versus time during the EK remediation using the modified EK reactor is illustrated in Figure 7. The control and test groups behave in a similar manner concerning the change in electric current (Figure 7A). Notwithstanding, the EOF of the test groups increases very quickly compared to that of the control group, implying that precipitation surrounding the cathode is eased using the ERSA system (Figure 7B). The Cu and Pb remediation efficiency following the EK remediation is presented in Figure 8. The highest Cu remediation efficiency of 78.8% is attained using the EKG electrode with graphene, while the highest Pb remediation efficiency of approximately 59.6% is attained using the same approach. Furthermore, the EK remediation using the EKG electrode performs the worst among the three approaches, most likely because of the formation of precipitation surrounding the cathode. These results indicate that the accumulated EOF is the main cause leading to an improvement in the remediation efficiency rather than the electric current. The higher the accumulated EOF, the larger the number of heavy metals migrated, and the higher the remediation efficiency.

In summary, although the EKG electrode can ease the effect of electrode polarization and aggravate the discharge of

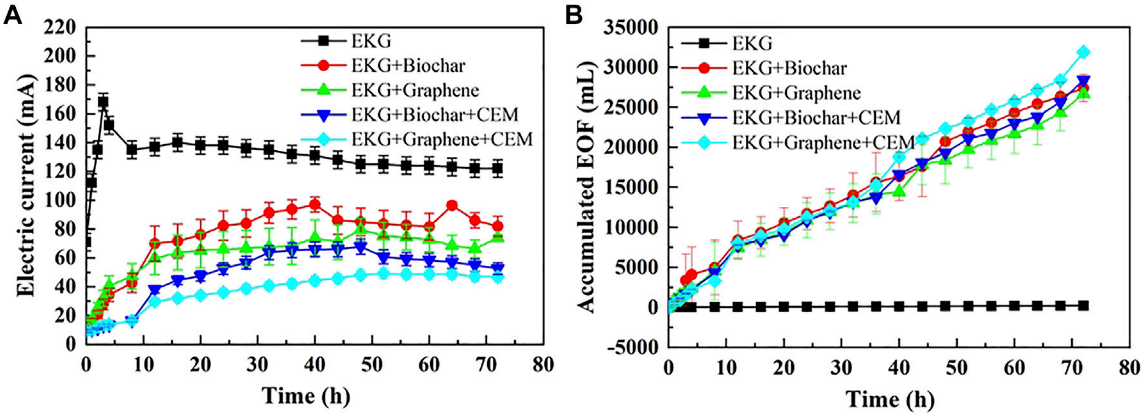

FIGURE 10
Variation of electric current and EOF versus time during the electrokinetic experiment subjected to the effect of the different treatments: **(A)** electric current and **(B)** accumulated EOF.

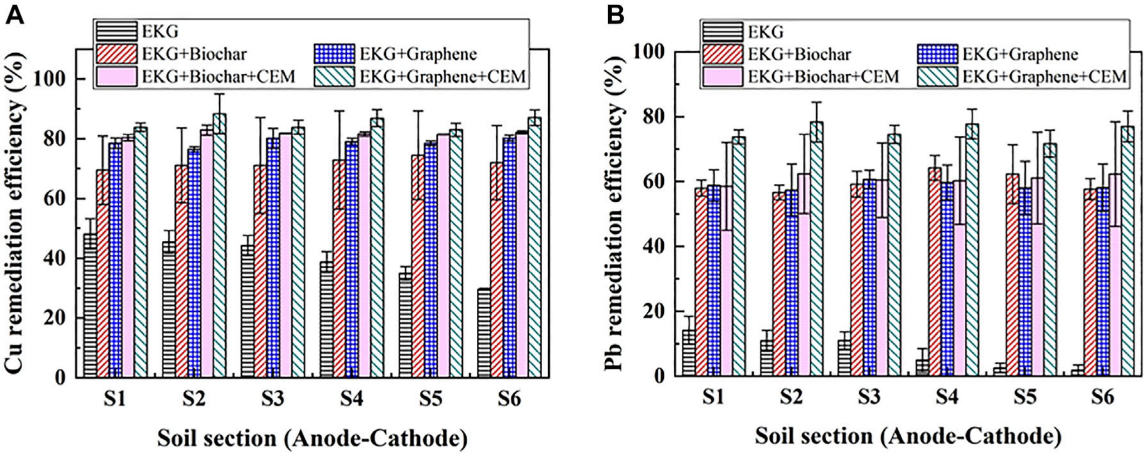

FIGURE 11
Removal of Cu and Pb after the electrokinetic experiment subjected to the effect of the different treatments: **(A)** Cu and **(B)** Pb.

H^+ and OH^- in the EK remediation, there is a significant shortcoming concerning the formation of precipitation surrounding the cathode, thereby reducing the remediation efficiency. The ERSA system is considered effective in mitigating the formation of precipitation where the electrolyte extracting from the anode cell and injecting into the cathode cell reduces the pH surrounding the cathode. The lower the pH surrounding the cathode, the more unlikely the formation of precipitation, and the higher desorption possibility of Cu^{2+} and Pb^{2+}. This is considered as the main cause leading to the highest remediation efficiency while using a combination of the EKG electrode and graphene.

3.3 Effect of cation exchange membrane

The variations of pH and EC against six soil sections under the CEM effect are presented in Figure 9. The use of CEM not only prevents a migration of OH^- to the specimen, but also further reduces pH over the entire specimen. In light of this, EC uses a combination of EKG and graphene as well as CEM that is higher compared to EC either using EKG or using a combination of EKG and graphene. A higher EC causes the electric current to go higher, leading to a higher EOF (Figure 10A). It is worth noting that the highest electric current is attained using EKG, while the lowest electric current is attained via a combination of EKG and graphene as well as CEM. This contradicts the above

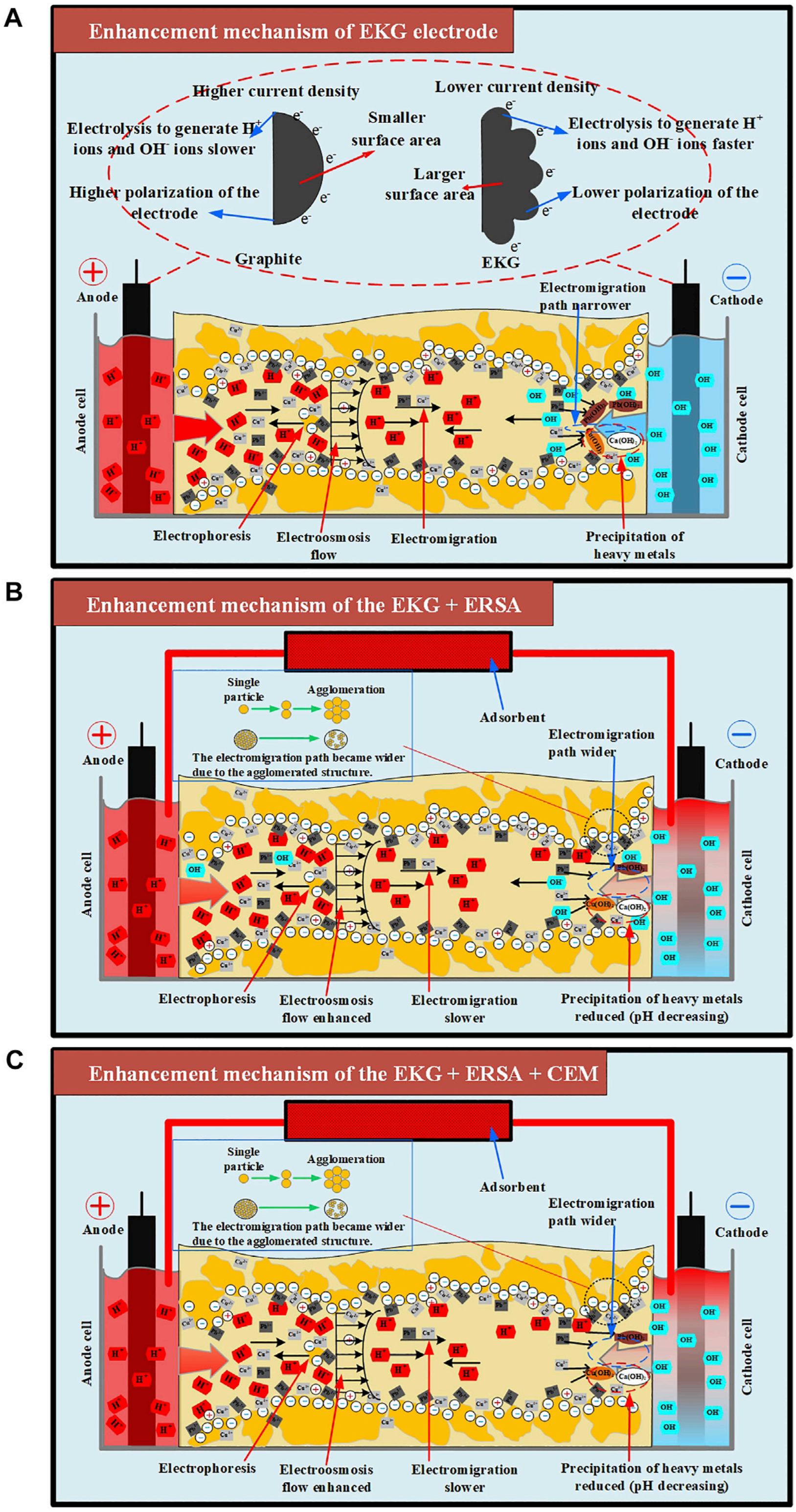

FIGURE 12
The enhancement mechanisms for Cu and Pb removal in loess: **(A)** enhancement mechanism of EKG electrode, **(B)** enhancement mechanism of the EKG + ERSA, **(C)** enhancement mechanism of the EKG + ERSA + CEM.

argument. This is because although the use of ERSA system can ease the formation of precipitation surrounding the cathode, it also circulates the anodic electrolyte to the cathode cell toward reducing the number of ions and causing a reduction in the electric current. In contrast, the number of ions in the anodic electrolyte does not show a drop when the ERSA system is neglected in the EK remediation, causing the highest electric current. The lower pH reduces the zeta potential and causes the formation of agglomerated structure toward lifting up the EOF (Figure 10B). The highest EOF is attained using a combination of EKG and ERSA (graphene), as well as CEM, most likely because of a reduction in the heavy metal precipitation, induced by the higher graphene's adsorption capacity. The variations of Cu and Pb remediation efficiency against six soil sections are shown in Figures 11A,B respectively. Overall, the Cu remediation efficiency is higher than the Pb remediation efficiency. Furthermore, the remediation efficiency using the modified EK reactor can be ordered as follows: EKG < EKG + ERSA (Biochar) < EKG + ERSA (Graphene) < EKG + ERSA (Biochar)+CEM < EKG + ERSA (Graphene)+CEM.

4 Discussion

It is well known that electric current flows through electrodes, leading to the polarization of the anode and cathode (Yuan et al., 2017; Wang et al., 2021). In this study, the use of graphite electrodes reduces not only the electric current, but also the EOF because of its polarization (Figure 4). Compared to the graphite electrode, the EKG electrode has a larger SSA and lower current density, and therefore, the migration of heavy metals is faster (Figure 12A). The discharge of H^+ and OH^- from the anode and cathode, respectively, is faster. This also indicates the faster acidification of the soil surrounding the anode and the faster precipitation surrounding the cathode. Therefore, the EKG electrode outperforms the graphite electrode regarding the removal of Cu and Pb (Figure 5).

Previous studies have emphasized the formation of precipitation surrounding the cathode. It impedes the development of electric current and then EOF toward degrading the remediation efficiency. To tackle such difficulty, the ERSA system was applied in this work to mitigate the formation of precipitation by circulating the anodic electrolyte to the cathode cell (Figure 12B). The pH surrounding the cathode was reduced as a result, preventing the formation of precipitation from occurring (Figure 6A). To this end, desorption of the heavy metals becomes easier than before, and an agglomerated structure can be formed because of the reduced pH surrounding. The agglomerated structure widens the electromigration path and indicates a higher EOF and a better remediation efficiency (Figures 7B, 8).

Although the ERSA use of is considered effective in reducing pH over the entire specimen, the formation of precipitation surrounding the cathode because of the soil alkalization remains to be addressed. In the present work, the use of CEM aims to further address the said issue by preventing the migration of OH^- to the specimen from the cathode (Figure 12C). A reduction in pH surrounding the cathode provides testimony regarding the above argument (Figure 9A). The smaller number of OH^- migrated, the lower potential of the formation of precipitation, and the higher the remediation efficiency. The thinner diffuse double layer, induced by the reduced pH, decreases the tortuosity of the electromigration path of cations and heavy metal ions. This also increases the electric current and EOF, indicating an improvement in the remediation efficiency (Figures 10, 11).

Overall, the use of EKG tackles the effect of electrode polarization. However, the effect of soil alkalization surrounding the cathode remains to be addressed. The ERSA system applied to the present work satisfactorily addresses the effect of soil alkalization surrounding the cathode by circulating the electrolyte from the anode cell to the cathode cell. Notwithstanding, the migration of OH^- to the specimen still causes some difficulty in easing the formation of precipitation surrounding the cathode. The combination of EKG electrode and ERSA, as well as CEM, is applied to the EK remediation and found to be effective in tackling the said problems (i.e., soil alkalization and heavy metal precipitation). The remediation efficiency as high as >85% verifies the applicability of the combination of EKG electrode and ERSA system, as well as CEM. The findings shed light on the potential of applying the EK technology in contaminated site remediation.

5 Conclusion

This study investigated the underlying mechanisms affecting the Cu and Pb remediation using the EK technology. The modified EK reactor was considered effective in improving the removal of Cu and Pb. Based on the results and discussion, some main conclusions can be drawn as follows:

1) The EKG electrode has a larger SSA and a lower current density, preventing the effect of electrode polarization and causing higher electric current. This further increases the EOF and causes an improvement in the removal of Cu and Pb. Notwithstanding, the formation of heavy metal precipitation surrounding the cathode still has to be addressed.
2) The ERSA system aims to reduce pH surrounding the cathode by circulating the anodic electrolyte to the cathode cell. The reduced pH eases the formation of heavy metal precipitation. The same reason also indicates easier desorption of Cu^{2+} and Pb^{2+} and a formation of the agglomerated structure. The agglomerated structure not only widens the electromigration

path, but indicates a higher EOF and better remediation efficiency.

3) The use of CEM intends to prevent the migration of OH^- to the specimen, thereby attaining the lowest pH and tackling the formation of precipitation surrounding the cathode. Such very low pH causes the diffuse double layer to become even thinner and decreases the tortuosity of the electromigration path of cations and heavy metal ions, indicating an increase in the electric current and EOF and improvement in the remediation efficiency. These results stand out as the relative merits of the modified EK reactor, namely, mitigating the effect of electrode polarization and easing the heavy metal precipitation surrounding the cathode. The findings shed light on the potential of applying the modified EK reactor to remedying the Cu- and Pb-rich water bodies.

Data availability statement

The original contributions presented in the study are included in the article/supplementary material, further inquiries can be directed to the corresponding author.

Author contributions

WH: data curation, formal analysis, validation, software, writing—original draft. W-CC: conceptualization, methodology, writing—review and editing, supervision, funding acquisition. SW: data curation, formal analysis, validation, software, writing—original draft. NK: formal analysis, validation, software.

Funding

This work would not have been possible without support from the Special Fund for Xi'an Key Laboratory of Geotechnical and Underground Engineering, Xi'an University of Science and Technology, under Grant no. XKLGUEKF20-02.

Conflict of interest

The authors declare that the research was conducted in the absence of any commercial or financial relationships that could be construed as a potential conflict of interest.

Publisher's note

References

Acar, Y. B., and Alshawabkeh, A. N. (1993). Principles of electrokinetic remediation. *Environ. Sci. Technol.* 27, 2638–2647. doi:10.1021/es00049a002

Bai, B., Nie, Q. K., Zhang, Y. K., Wang, X. L., and Hu, W. (2021a). Cotransport of heavy metals and SiO_2 particles at different temperatures by seepage. *J. Hydrology* 597, 125771. doi:10.1016/j.jhydrol.2020.125771

Bai, B., Xu, T., Nie, Q. K., and Li, P. P. (2020). Temperature-driven migration of heavy metal Pb^{2+} along with moisture movement in unsaturated soils. *Int. J. Heat Mass Transf.* 153, 119573. doi:10.1016/j.ijheatmasstransfer.2020.119573

Bai, B., Yang, G. C., Li, T., and Yang, G. S. (2019). A thermodynamic constitutive model with temperature effect based on particle rearrangement for geomaterials. *Mech. Mater.* 139, 103180. doi:10.1016/j.mechmat.2019.103180

Bai, X. D., Cheng, W. C., and Li, G. (2021b). A comparative study of different machine learning algorithms in predicting EPB shield behaviour: A case study at the xi'an metro, China. *Acta Geotech.* 16 (12), 4061–4080. doi:10.1007/s11440-021-01383-7

Bai, X. D., Cheng, W. C., Sheil, B. B., and Li, G. (2021c). Pipejacking clogging detection in soft alluvial deposits using machine learning algorithms. *Tunn. Undergr. Space Technol.* 113, 103908. doi:10.1016/j.tust.2021.103908

Baker, B., Maria, E., and Adel, H. (2018). Electrokinetic nondestructive *in-situ* technique for rehabilitation of liners damaged by fuels. *J. Hazard. Mater.* 359, 510–515. doi:10.1016/j.jhazmat.2018.07.113

Bala, R. P., Srivastava, R. K., and Mohan, D. (2015). Electrokinetic removal of mixed heavy metals from a contaminated low permeable soil by surfactant and chelants. *Environ. Earth Sci.* 73 (3), 1191–1204. doi:10.1007/s12665-014-3474-4

Begum, W., Rai, S., Banerjee, S., Bhattacharjee, S., Mondal, M. H., Bhattarai, A., et al. (2022). A comprehensive review on the sources, essentiality and toxicological profile of nickel. *RSC Adv.* 12, 9139–9153. doi:10.1039/d2ra00378c

Beyrami, H. (2020). Effect of different treatments on electrokinetic remediation of Zn, Pb and Cd from a contaminated calcareous soil. *Chin. J. Chem. Eng.* 38, 255–265. doi:10.1016/j.cjche.2020.09.011

Bilal, M., Shah, J. A., Ashfaq, T., Gardazi, S. M. H., Tahir, A. A., Pervez, A., et al. (2013). Waste biomass adsorbents for copper removal from industrial wastewater—a review. *J. Hazard. Mater.* 263, 322–333. doi:10.1016/j.jhazmat.2013.07.071

Caparrós, P. G., Ozturk, M., Gul, A., Batool, T. S., Anosheh, H. P., Unal, B. T. I., et al. (2022). Halophytes have potential as heavy metal phytoremediators: A comprehensive review. *Environ. Exp. Bot.* 193, 104666. doi:10.1016/j.envexpbot.2021.104666

Chang, J. H., Wang, Y. L., and Shen, S. Y. (2018). A specific configuration of circulation-enhanced electrokinetics (CEEK) to remediate real-site Cd and Pb contaminated soils. *J. Hazard. Mater.* 359, 408–413. doi:10.1016/j.jhazmat.2018.07.079

Chen, X. Y., Kumari, D., Cao, C. J., Grazyna, P., and Varenyam, A. (2020). A review on remediation technologies for nickel-contaminated soil. *Hum. Ecol. Risk Assess. Int. J.* 26 (3), 571–585. doi:10.1080/10807039.2018.1539639

Ding, D., Song, X., Wei, C., and La, C. J. (2019). A review on the sustainability of thermal treatment for contaminated soils. *Environ. Pollut.* 253, 449–463. doi:10.1016/j.envpol.2019.06.118

Du, Y. J., Jin, F., Liu, S. Y., Chen, L., and Zhang, F. (2011). Review of stabilization/solidification technique for remediation of heavy metals contaminated lands. *Rock Soil Mech.* 32 (1), 116–124.

Duan, Z., Cheng, W. C., Peng, J. B., and Tang, H. (2021). Interactions of landslide deposit with terrace sediments: Perspectives from velocity of deposit movement and apparent friction angle. *Eng. Geol.* 280, 105913. doi:10.1016/j.enggeo.2020.105913

Fan, G. P., Zhang, Z. H., Ai, Y. C., Gao, Y., Zhou, D. M., Cang, L., et al. (2021). Electrokinetical enhanced delivery of acidic potassium permanganate and removal of copper-pyrene compound pollution in a red soil. *Chemosphere* 263, 128085. doi:10.1016/j.chemosphere.2020.128085

Garcia-Sanchez, M., Kosnar, Z., Mercl, F., Aranda, E., and Tlustos, P. (2018). A comparative study to evaluate natural attenuation, mycoaugmentation, phytoremediation, and microbial-assisted phytoremediation strategies for the bioremediation of an aged PAH-polluted soil. *Ecotoxicol. Environ. Saf.* 147 (1), 165–174. doi:10.1016/j.ecoenv.2017.08.012

Ghosh, D., Saha, R., Ghosh, A., Nandi, R., and Saha, B. (2015). A review on toxic cadmium biosorption from contaminated wastewater. *Desalination Water Treat.* 53 (2), 413–420. doi:10.1080/19443994.2013.846233

Han, D., Wu, X. Y., Tang, X. Q., Xiao, S. B., and Scholz, M. (2021). Critical review of electro-kinetic remediation of contaminated soils and sediments: Mechanisms, performances and technologies. *Water Air Soil Pollut.* 232, 335. doi:10.1007/s11270-021-05182-4

He, T., Xu, Z. J., Wang, J. F., Wang, F. P., Zhou, X. F., Wang, L. L., et al. (2022). Improving cadmium accumulation by Solanum nigrum L. via regulating rhizobacterial community and metabolic function with phosphate-solubilizing bacteria colonization. *Chemosphere* 287, 132209. doi:10.1016/j.chemosphere.2021.132209

Hu, W. L., Cheng, W. C., Wang, L., and Xue, Z. F. (2022a). Micro-structural characteristics deterioration of intact loess under acid and saline solutions and resultant macro-mechanical properties. *Soil Tillage Res.* 220, 105382. doi:10.1016/j.still.2022.105382

Hu, W. L., Cheng, W. C., and Wen, S. J. (2022b). Investigating the effect of degree of compaction, initial water content, and electric field intensity on electrokinetic remediation of an artificially Cu- and Pb-contaminated loess. *Acta Geotech.* doi:10.1007/s11440-022-01602-9

Hu, W. L., Cheng, W. C., Wen, S. J., and Rahman, M. M. (2021a). Effects of chemical contamination on microscale structural characteristics of intact loess and resultant macroscale mechanical properties. *Catena* 203, 105361. doi:10.1016/j.catena.2021.105361

Hu, W. L., Cheng, W. C., Wen, S. J., and Yuan, K. (2021b). Revealing the enhancement and degradation mechanisms affecting the performance of carbonate precipitation in EICP process. *Front. Bioeng. Biotechnol.* 9, 750258. doi:10.3389/fbioe.2021.750258

Kalantari, B., and Prasad, A. (2014). A study of the effect of various curing techniques on the strength of stabilized peat. *Transp. Geotech.* 1 (3), 119–128. doi:10.1016/j.trgeo.2014.06.002

Kim, W. S., Kim, S. O., and Kim, K. W. (2005). Enhanced electrokinetic extraction of heavy metals from soils assisted by ion exchange membranes. *J. Hazard. Mater.* B118, 93–102. doi:10.1016/j.jhazmat.2004.10.001

Li, C., Hou, H. J., Yang, J. K., Liang, S., Shi, Y. F., Guan, R. N., et al. (2019). Comparison of electrokinetic remediation on lead-contaminated kaolinite and natural soils. *Clean. –. Soil Air Water* 47 (4), 1800337. doi:10.1002/clen.201800337

Ling, J. M., Li, X., Qian, J. S., and Li, X. Y. (2021). Performance comparison of different electrode materials for electroosmosis treatment on subgrade soil. *Constr. Build. Mater.* 271, 121590. doi:10.1016/j.conbuildmat.2020.121590

Liu, H., Li, J. B., Zhao, M., Li, Y. B., and Chen, Y. M. (2019). Remediation of oil-based drill cuttings using low-temperature thermal desorption: Performance and kinetics modeling. *Chemosphere* 235, 1081–1088. doi:10.1016/j.chemosphere.2019.07.047

Liu, K. H., Guan, X. J., Li, C. M., Zhao, K. Y., Yang, X. H., Fu, R. X., et al. (2022). Global perspectives and future research directions for the phytoremediation of heavy metal-contaminated soil: A knowledge mapping analysis from 2001 to 2020. *Front. Environ. Sci. Eng.* 16 (6), 73. doi:10.1007/s11783-021-1507-2

Liu, T., Yuan, X. X., Zhang, G., Hu, J., An, J., and Chen, T. (2020). Stir bar sorptive extraction and automatic two-stage thermal desorption-gas chromatography-mass spectrometry for trace analysis of the byproducts from diphenyl carbonate synthesis. *Microchem. J.* 153, 104341. doi:10.1016/j.microc.2019.104341

Lu, C., Hong, Y., Liu, J., Gao, Y. Z., Ma, Z., Yang, B., et al. (2019b). A PAH-degrading bacterial community enriched with contaminated agricultural soil and its utility for microbial bioremediation. *Environ. Pollut.* 251, 773–782. doi:10.1016/j.envpol.2019.05.044

Lu, Y. S., Wang, W. B., Wang, Q., Xu, J., and Wang, A. Q. (2019a). Effect of oxalic acid-leaching levels on structure, color and physico-chemical features of palygorskite. *Appl. Clay Sci.* 183, 105301. doi:10.1016/j.clay.2019.105301

Meseldzija, S., Petrovic, J., Onjia, A., Volkov-Husovic, T., Nesic, A., Vukelic, N., et al. (2019). Utilization of agro-industrial waste for removal of copper ions from aqueous solutions and mining-wastewater. *J. Industrial Eng. Chem.* 75, 246–252. doi:10.1016/j.jiec.2019.03.031

Ministry of Water Resources of the People's Republic of China (2019). *Standard for geotechnical test methods, GB/T 50123-2019*. Beijing: China Planning Press.

Mohamadi, S., Saeedi, M., and Mollahosseini, A. (2019). Enhanced electrokinetic remediation of mixed contaminants from a high buffering soil by focusing on mobility risk. *J. Environ. Chem. Eng.* 7 (6), 103470. doi:10.1016/j.jece.2019.103470

Muddanna, M. H., and Baral, S. S. (2019). A comparative study of the extraction of metals from the spent fluid catalytic cracking catalyst using chemical leaching and bioleaching by Aspergillus Niger. *J. Environ. Chem. Eng.* 7 (5), 103335. doi:10.1016/j.jece.2019.103335

Mukherjee, K., Saha, R., Ghosh, A., and Saha, B. (2013). Chromium removal technologies. *Res. Chem. Intermed.* 39, 2267–2286. doi:10.1007/s11164-012-0779-3

Mwandira, W., Nakashima, K., and Kawasaki, S. (2017). Bioremediation of lead-contaminated mine waste by Pararhodobacter sp. based on the microbially induced calcium carbonate precipitation technique and its effects on strength of coarse and fine grained sand. *Ecol. Eng.* 109, 57–64. doi:10.1016/j.ecoleng.2017.09.011

National Bureau of Statistics (2001). *China statistical Yearbook*. Beijing, China: China National Publishing House.

National Bureau of Statistics (2018). *China Statistical Yearbook*. Beijing, China: China National Publishing House.

Saha, B., and Orvig, C. (2010). Biosorbents for hexavalent chromium elimination from industrial and municipal effluents. *Coord. Chem. Rev.* 254, 2959–2972. doi:10.1016/j.ccr.2010.06.005

Saha, R., Nandi, R., and Saha, B. (2011). Sources and toxicity of hexavalent chromium. *J. Coord. Chem.* 64 (10), 1782–1806. doi:10.1080/00958972.2011.583646

Puppala, S. K., Alshawabkeh, A. N., Acar, Y. B., Gale, R. J., and Bricka, M. (1997). Enhanced electrokinetic remediation of high sorption capacity soil. *J. Hazard. Mater.* 55 (1–3), 203–220. doi:10.1016/s0304-3894(97)00011-3

Tak, H. I., Ahmad, F., and Babalola, O. (2013). Advances in the application of plant growth-promoting rhizobacteria in phytoremediation of heavy metals. *Rev. Environ. Contam. Toxicol.* 223, 33–52. doi:10.1007/978-1-4614-5577-6_2

Wang, F., Shen, Z. T., Liu, R. Q., Zhang, Y. H., Xu, J., Al-Tabbaa, A., et al. (2019). GMCs stabilized/solidified Pb/Zn contaminated soil under different curing temperature: Physical and microstructural properties. *Chemosphere* 239, 124738. doi:10.1016/j.chemosphere.2019.124738

Wang, L., Cheng, W. C., and Xue, Z. F. (2022a). Investigating microscale structural characteristics and resultant macroscale mechanical properties of loess exposed to alkaline and saline environments. *Bull. Eng. Geol. Environ.* 81, 146. doi:10.1007/s10064-022-02640-z

Wang, L., Cheng, W. C., and Xue, Z. F. (2022b). The effect of calcium source on Pb and Cu remediation using enzyme-induced carbonate precipitation. *Front. Bioeng. Biotechnol.* 10, 849631. doi:10.3389/fbioe.2022.849631

Wang, L. Q., Shao, S. J., and She, F. T. (2020). A new method for evaluating loess collapsibility and its application. *Eng. Geol.* 264, 105376. doi:10.1016/j.enggeo.2019.105376

Wang, Y. C., Li, A., and Cui, C. W. (2021). Remediation of heavy metal-contaminated soils by electrokinetic technology: Mechanisms and applicability. *Chemosphere* 265, 129071. doi:10.1016/j.chemosphere.2020.129071

Wen, D. D., Fu, R. B., and Li, Q. (2021). Removal of inorganic contaminants in soil by electrokinetic remediation technologies: A review. *J. Hazardous Materials* 401, 123345.

Wu, Y. J., Santos, S. S., Vestergård, M., González, A. M. M., Ma, L. Y., Feng, Y., et al. (2022). A field study reveals links between hyperaccumulating Sedum plants-associated bacterial communities and Cd/Zn uptake and translocation. *Sci. Total Environ.* 805, 150400. doi:10.1016/j.scitotenv.2021.150400

Xu, H. T., Song, Y., Cang, L., and Zhou, D. M. (2020). Ion exchange membranes enhance the electrokinetic *in situ* chemical oxidation of PAH-contaminated soil. *J. Hazard. Mater.* 382, 121042. doi:10.1016/j.jhazmat.2019.121042

Xue, Z. F., Cheng, W. C., and Wang, L. (2021b). Effect of straw reinforcement on the shearing and creep behaviours of Quaternary loess. *Sci. Rep.* 11, 19926. doi:10.1038/s41598-021-99318-5

Xue, Z. F., Cheng, W. C., Wang, L., and Hu, W. L. (2022). Effects of bacterial inoculation and calcium source on microbial-induced carbonate precipitation for lead remediation. *J. Hazard. Mater.* 426, 128090. doi:10.1016/j.jhazmat.2021.128090

Xue, Z. F., Cheng, W. C., Wang, L., and Song, G. Y. (2021a). Improvement of the shearing behaviour of loess using recycled straw fiber reinforcement. *KSCE J. Civ. Eng.* 25, 3319–3335. doi:10.1007/s12205-021-2263-3

Yuan, L. Z., Xu, X. J., Li, H. Y., Wang, Q. Y., Wang, N. N., Yu, H. W., et al. (2017). The influence of macroelements on energy consumption during periodic power electrokinetic remediation of heavy metals contaminated black soil. *Electrochimica Acta* 235, 604–612. doi:10.1016/j.electacta.2017.03.142

Zang, F., Wang, S. L., Nan, Z. R., Zhao, C. Y., Sun, H. L., Huang, W., et al. (2019). Leachability of heavy metals in loess-amended dredged sediment from Northwest of China. *Ecotoxicol. Environ. Saf.* 183, 109561. doi:10.1016/j.ecoenv.2019.109561

Zeng, X. Y., Li, S. W., Leng, Y., and Kang, X. H. (2020). Structural and functional responses of bacterial and fungal communities to multiple heavy metal exposure in arid loess. *Sci. Total Environ.* 723, 138081. doi:10.1016/j.scitotenv.2020.138081

Zheng, R. J., Feng, X. Z., Zou, W. S., Wang, R. H., Yang, D. Z., Wei, W. F., et al. (2021). Converting loess into zeolite for heavy metal polluted soil remediation based on "soil for soil-remediation" strategy. *J. Hazard. Mater.* 412, 125199. doi:10.1016/j.jhazmat.2021.125199

Zhou, H. D., Liu, Z. Y., Li, X., and Xu, J. H. (2021). Remediation of lead (II)-contaminated soil using electrokinetics assisted by permeable reactive barrier with different filling materials. *J. Hazard. Mater.* 408, 124885. doi:10.1016/j.jhazmat.2020.124885

Zhou, R., Liu, X. C., Luo, L., Zhou, Y. Y., Wei, J. H., Chen, A. W., et al. (2017). Remediation of Cu, Pb, Zn and Cd-contaminated agricultural soil using a combined red mud and compost amendment. *Int. Biodeterior. Biodegrad.* 118, 73–81. doi:10.1016/j.ibiod.2017.01.023

Zhu, C. P., Liu, H. L., and Shen, Y. (2011). Laboratory tests on shear strength properties of soil polluted by acid and alkali. *Chin. J. Geotechnical Eng.* 33 (7), 164–170.

Zu, Y., Yuan, L., Schvartz, C., Langlade, L., and Fan, L. (2004). Accumulation of Pb, Cd, Cu and Zn in plants and hyperaccumulator choice in Lanping lead-zinc mine area, China. *Environ. Int.* 30, 567–576. doi:10.1016/j.envint.2003.10.012